Materials Today: Proceedings 42 (2021) 3089–3096

Contents lists available at ScienceDirect

Materials Today: Proceedings

journal homepage: www.elsevier.com/locate/matpr

Accuracy investigation of 3D printed PLA with various process parameters and different colors

Muammel M. Hanon [a,b,*], László Zsidai [a], Quanjin Ma [c]

[a] Mechanical Engineering Doctoral School, Szent István University, Gödöllő 2100, Hungary
[b] Baquba Technical Institute, Middle Technical University (MTU), Baghdad, Iraq
[c] Structural Materials & Degradation Focus Group, Faculty of Mechanical & Automotive Engineering Technology, Universiti Malaysia Pahang, 26600 Pekan, Pahang, Malaysia

ARTICLE INFO

Article history:
Received 11 November 2020
Received in revised form 4 December 2020
Accepted 13 December 2020
Available online 28 February 2021

Keywords:
Additive manufacturing (AM)
Fused deposition modeling (FDM)
Print process parameters
Polylactic acid (PLA)
Dimensional accuracy
Weight precision

ABSTRACT

The accuracy of three-dimensional (3D) printing is how the dimensions of a measured product are close to its original model's nominal values. Thus, dimensional accuracy is essential for determining the machine's reliability to produce each object according to the expected results. In this study, the influence of 3D printing process parameters on the dimensional accuracy of specimens manufactured using Polylactic acid (PLA) material is investigated. Based on fused deposition modeling (FDM) technology, cylindrical and dog-bone tensile test samples are fabricated at various process parameters, including build orientation, raster direction angle, and layer thickness. PLA filaments with three different colors (white, grey, and black) are utilized to produce the required test pieces. The dimensional accuracy for cylindrical (diameter and length) and dog-bone (width and thickness) samples have been evaluated. The nominal values are considered the reference to determine the accuracy percentage for each specimen. The weight of all test pieces is also examined, and its precision is assessed. The optimum process parameter settings have been defined to minimize the error percentage in the dimensions of the printed parts. According to the results, a high overall dimensional accuracy of 98.81% was achieved, which indicates the ability of commercial FDM 3D printers as an inexpensive and decent quality alternative for producing utilitarian parts. The filament's color displayed a notable impact on the test pieces' weight, where the difference between the heaviest (white) and lightest (black) specimens is almost a percentage of 7.24%. A remarkable influence was noticed for the layer thickness parameter on the accuracy, meanwhile the raster direction angle parameter appeared no effect when the number of layers and the contour size are the same. The data obtained from this study might help identify the optimum configurations that guide the production of components using thermoplastic filaments through FDM 3D printing.

1. Introduction

3D printing is a modern technology that provides various new possibilities for complex-shaped objects to be made. It helps designers, based on a CAD model, to build real objects [1]. This technology is already making a significant impact in numerous fields such as industry, agriculture, and medicine [2–5]. Fused deposition modeling (FDM) is one of the most common additive manufacturing techniques, comprising extrusion of thermoplastic filaments for deposition as layer by layer [6]. Among other thermoplastic (filaments) materials utilized in the FDM technique, ABS, PLA, PETG, and PC are the most popular ones [7–10]. The mechanical properties of FDM printed components are significantly influenced by the design and processing conditions of the process, often exhibiting anisotropic mechanical properties due to the choice of specific orientation of the infill layer [11]. The effect of the FDM process parameters on the mechanical properties of fabricated parts was extensively investigated in the literature [12–16]. However, only limited research yet have studied the dimensional accuracy of FDM 3D printing and the impact of the process settings on it.

Hyndhavi et al. used grey relational grade analysis to determine the optimum parameters of the employed settings for minimizing the error percentage in length, width, and thickness of the exam-

* Corresponding author at: Mechanical Engineering Doctoral School, Szent István University, Gödöllő 2100, Hungary.
E-mail address: Sharba.Muammel.M.Hanon@phd.uni-szie.hu (M.M. Hanon).

https://doi.org/10.1016/j.matpr.2020.12.1246
2214-7853/

ined parts. Based on the obtained results, the layer thickness of 200 μm, raster direction of 0° angle, and build orientation of 0 and 90°are the best parameters to refine the overall dimensional accuracy. As they concluded that the specimens fabricated using Acrylonitrile Butadiene Styrene (ABS) material exhibited higher accuracy than PLA material [17]. In contrast, Alsoufi et al. showed that the height dimension of ABS test pieces displayed the worst shape error reached almost a maximum percentage of 34.53% comparing to the base model. They examined the dimensional accuracy of FDM 3D printed PLA, PLA+, ABS, and ABS + thermoplastics in rectangular form specimens. This high shape error percentage in the ABS samples was attributed to undesirable warping deformation that occurs as a result of heat shrinkage. Though, the lowest warping deformation in the height dimension was represented by a shape error of 1.47% and 1.33% for PLA and PLA + materials, respectively. In terms of length and width dimensions, PLA + revealed the best accuracy with a minimum shape error of 0.05% [18]. Zhang et al. compared between the accuracies of dental models manufactured utilizing digital light processing (DLP) and stereolithography (SLA) 3D printing techniques at different thicknesses. The layer thicknesses were ranged from 20 μm to 100 μm when producing all printed dental pieces (22 models). They stated that higher printing accuracy for DLP technology was detected at a layer thickness of 100 μm. Nevertheless, when using SLA technology the printing accuracy increases as the layer thickness decreased [19]. Nuñez et al. studied the dimensional accuracy obtained in FDM 3D printing with ABS + as the model material. They have used two layer thicknesses (0.178 mm and 0.254 mm) and two densities (low and solid) in the experimental tests. They found out that the best dimensional accuracy behavior was observed with the maximum layer thickness of (0.254 mm) and the solid density (100% infill) with a maximum deviation of 36 μm [20].

It can be recognized from the previous works mentioned above that most researchers paid attention to study the accuracy of rectangular shape 3D printed specimens. This work aims to determine the influence of various process settings on the dimensional accuracy of 3D printed objects in cylindrical and rectangular forms. Furthermore, to study the effect of these process settings as well as filament colors on the weight precision of the printed parts, which was never studied elsewhere. To this end, FDM 3D printed specimens in the form of cylindrical and dog-bone tensile test pieces were produced to investigate the dimensional accuracy. The cylindrical samples were made with three different colors (white, grey, and black) and under various build orientation (Horizontal, 45° angle, and Vertical). At the same time, the dog-bone specimens were manufactured under three different print parameters (build orientation [Flat, On-edge, and Upright], raster direction angle [0/45°, 45/135°, and 45/90°], and layer thickness [100 μm, 200 μm, and 300 μm]). The dimensional accuracy of 3D printing is how the measured product (in terms of dimensions) close to the nominal value, where the nominal value reflects the CAD model's dimensions. Therefore, the achieved dimensional results (for cylindrical "diameter and length" and dog-bone "thickness and width" test pieces) were compared with the nominal values of each condition in order to obtain the accuracy percentage. Weighing for all manufactured specimens was carried out to discover whether various print settings and filament colors would affect the weight and its precision. This data is vital in additive manufacturing for determining the reliability of the machine. In other words, to count on the 3D printer to fabricate each product according to the required dimensions.

Table 1
Parameters used for printing test

Cylindrical specimens			Dog-bone tensile test specimens		
Color	Parameter	Settings	Color	Parameter	Settings
White	Print orientation	Horizontal	White	Print orientation	Flat
		45°			On-Edge
		Vertical			Upright
Grey		Horizontal		Raster direction angle	0/45°
		45°			45/135°
		Vertical			45/90°
Black		Horizontal		Layer thickness	100 μm
		45°			200 μm
		Vertical			300 μm

2. Materials and methods

2.1. Preparation of materials and 3D printing

Fused deposition modeling (FDM) technique was employed to fabricate the test specimens with the commercial 3D printer WANHAO Duplicator 6. This printer has a nozzle diameter of 0.4 mm and exists in the laboratory of additive manufacturing at Szent István University, Hungary. Polylactic Acid (PLA) filaments were purchased from the 3D printer material manufacturer eSUN. These filaments with a diameter of 1.75 mm and three different colors (white, gray, and black) were utilized for manufacturing samples. A three-dimensional designing software AutoCAD 2020, was used to generate the 3D CAD model of the sample and convert it to the ".STL" file format. In order to slice the STL file (3D model), Ultimaker Cura 4.3 software was employed. The file exported from the slicing software is the G-code since it is compatible with the 3D printer. The printing was performed at a temperature of 195 °C, and the platform was maintained at 60 °C.

2.2. Process parameters for producing specimens

Models printed were divided into two groups, including cylinders and dog-bone tensile test specimens. Parameters and settings used for printing the samples of these two groups are listed in Table 1. The cylindrical pieces were printed with three colors and at various build orientation (Horizontal, 45° angle, and Vertical) while raster direction angle and layer thickness were fixed at 45/135° and 200 μm, respectively (see Fig. 1 (a)). However, the doge-bone tensile specimens were produced at three print orientations (Flat, On-edge, and Upright), three raster direction angle (0/45°, 45/135°, and 45/90°), and three layer thickness (100 μm, 200 μm, and 300 μm), as illustrated in Fig. 1 (b). All printed parts were manufactured at 100% infill density. A physical appearance for the specimens after manufacturing is exhibited in Fig. 2 (a) and (b). It can be clearly seen that support materials were used due to the tilt in 45° angle cylindrical specimens. The cylindrical test specimens were 3D-printed with a diameter of 8 mm and a height of 15.2 mm. Meanwhile, the dog-bone tensile test pieces' geometry was produced according to the ISO 527–2: 2012 standard type 1B specimen [21] with dimensions of 150 mm by 20 mm by 4 mm.

2.3. Accuracy measurements procedure

The measurements were accomplished on the samples of both printed groups (cylindrical and dog-bone) in order to obtain accuracy and precision. The reason for choosing cylinders and dog-bone is to inspect 3D printed parts' accuracy in circular and rectangular shapes. Concerning the cylindrical test pieces, the dimensions (di-

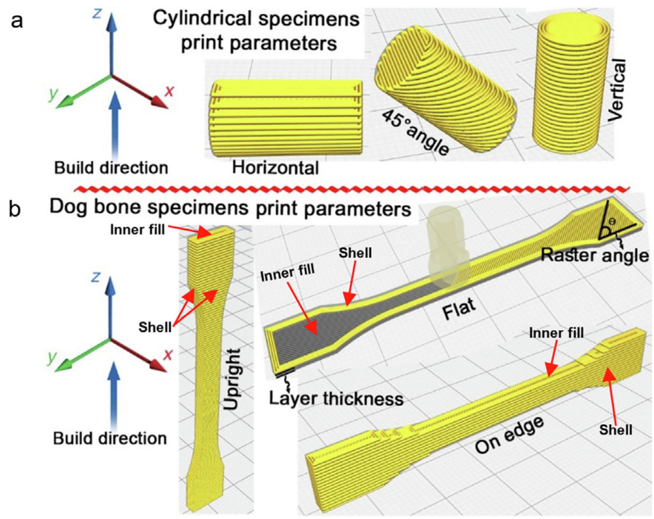

Fig. 1. (a) print orientations of cylindrical test specimens; (b) parameters used for printing dog-bone test specimens including print orientation, raster direction angle, and layer thickness.

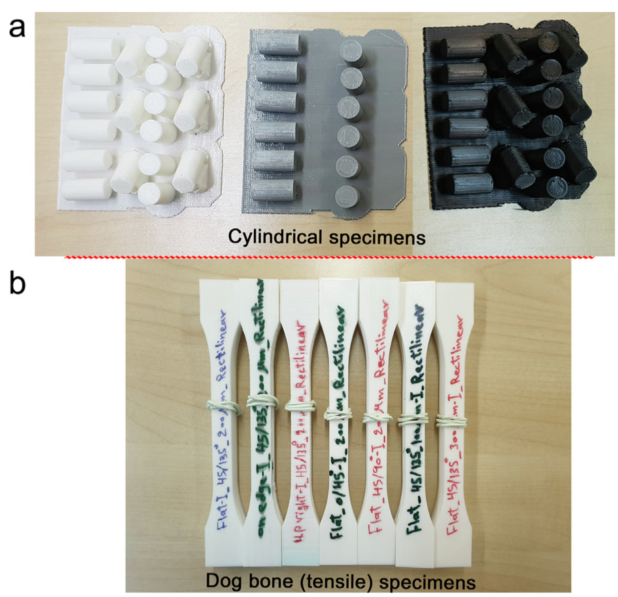

Fig. 2. (a) 3D-printed cylindrical specimens with different build orientations; (b) 3D-printed dog-bone tensile test specimens at various process parameters.

ameter and length) were measured for all samples. Fig. 3 (a) displays that length was measured at the marked points (three spots), whereas diameter was investigated in the X and Y direction from both ends of the cylinder. Regarding the dog-bone tensile test specimen, the gauge section is the most crucial part. The width (b) and thickness (h) (gauge cross-section) were measured at both ends of the section as well as the middle (total; three positions), as illustrated in Fig. 3 (b). Hence to determine the accuracy, the obtained dimensions results had to be compared with the original CAD design. For a precise evaluation, the same measuring mechanism has been applied on six identical samples (the same manufacturing condition) of the cylinders and three duplicate specimens of the dog-bone pieces. The precision (repeatability) was determined through the standard deviation calculations exhibited by error bars. All samples were weighed by a Sartorius scale (Sartorius Corporation, Gottingen, Germany), and its weight precision was checked as well.

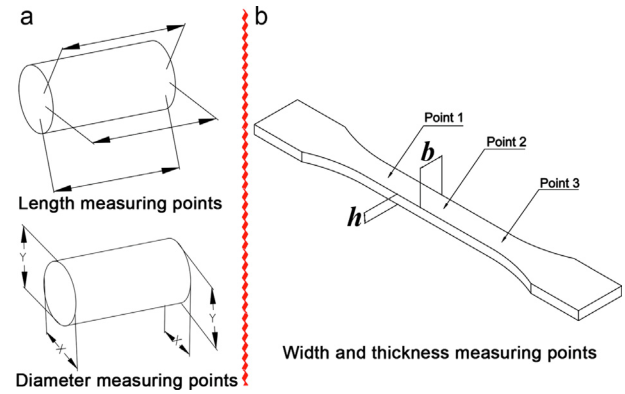

Fig. 3. (a) measurement positions for the length and diameter of cylindrical test samples; (b) measurement points for the width (b) and thickness (h) on the gauge section of the dog-bone tensile test specimen.

3. Results and discussion

3.1. Raw results evaluation

The dimensions for the cylindrical and dog-bone test specimens were measured using a digital Vernier caliper. The raw results obtained for dimensional measurement of cylindrical and dog-bone test samples are tabulated in Tables 2 and 3, respectively. As shown in Fig. 3 (a), the length was measured for the cylindrical specimens at three different points. In contrast, diameter measurements were done on the X and Y axis at both cylinder edges. The results were compared with the cylinder dimensions' nominal values: diameter of 8 mm and a length of 15.2 mm. In respect of the dog-bone tensile test pieces, the dimensions of width and thickness for each specimen were investigated at three points on the gauge area, as displayed in Fig. 3 (b). The gauge section dimensions' nominal values, including a width (b) of 10 mm and a thickness (h) of 4 mm, were used for the comparison to evaluate the accuracy. With regard to the weight accuracy calculations, there was no nominal value to compare with, as the slicing program does not display fractions at the amount provided for the sample shown in the original STL file. It only gives integer numbers such as 1 g for current cylindrical test samples and 8 g for the dog-bone ones, which are not accurate values. Thus, the average value for each print condition was taken, and it was considered the base value for comparison purposes with the results of the same group. The results presented in Tables 2 and 3 were averaged, and its accuracy percentage calculated. These accuracy percentage results with their standard deviation (SD) for cylindrical and dog-bone test samples are listed in Tables 4 and 5, respectively.

3.2. Accuracy of cylindrical test specimens

Fig. 4 shows a comparison among the dimensional (diameter and length) accuracy of cylindrical test specimens manufactured in different print orientation (Horizontal, 45° angle, and Vertical) and color (white, grey, and black). From Table 4 and Fig. 4, it can be clearly seen that the worst dimensional accuracy with elevated standard deviation error bar values was observed in the 45° angle specimens. This was expected due to layers positioning, as layers of this specimen were built tilted. Therefore, the possibility of distortion increases due to the influence of gravity throughout curing. Generally, most of the cylindrical samples showed a high accuracy percentage ranging between 98.36% and 99.72% in both diameter and length measurements compared to the nominal value. After overall calculations, a precision of 99.14% and 99.35% against the

Table 2
The raw results obtained from dimensional measurements of cylindrical test

Filament color	No.	Sample settings	First edge diameter X (mm)	First edge diameter Y (mm)	Second edge diameter X (mm)	Second edge diameter Y (mm)	Length L1 (mm)	Length L2 (mm)	Length L3 (mm)	Specimen weight (mg)
White	1	Horizontal I	8.05	8.06	8.09	8.03	15.28	15.21	15.25	814
	2	Horizontal II	8.19	8	7.97	7.99	15.33	15.21	15.23	814
	3	Horizontal III	8.16	7.97	8.1	8.03	15.29	15.16	15.23	819
	4	Horizontal IV	8.04	8.01	8.04	8	15.31	15.38	15.21	790
	5	Horizontal V	8.04	8.01	7.97	8.02	15.25	15.2	15.22	779
	6	Horizontal VI	8.13	8.01	8.09	8.01	15.37	15.26	15.26	812
	7	45° I	8	8.12	8.05	8.29	15.69	15.54	15.42	839
	8	45° II	7.97	7.82	8.01	8.18	15.46	15.35	15.23	830
	9	45° III	8.09	8.03	8.13	7.97	15.52	15.37	15.43	819
	10	45° IV	7.97	8.17	8.05	8.34	15.78	15.2	15.2	849
	11	45° V	7.93	8.4	8.05	8.51	15.63	15.59	15.49	841
	12	45° VI	7.99	8.03	8.2	8.07	15.48	15.4	15.41	837
	13	Vertical I	8.05	8.09	8.09	8.09	15.25	15.29	15.28	814
	14	Vertical II	8.03	8.07	8.11	8.01	15.2	15.31	15.29	813
	15	Vertical III	8	8.06	8.06	8.08	15.26	15.29	15.24	798
	16	Vertical IV	8.04	8.07	8.01	8.03	15.27	15.24	15.25	788
	17	Vertical V	8.1	8.09	8.06	8.03	15.24	15.26	15.26	799
	18	Vertical VI	8.13	8.12	8.11	8.12	15.27	15.24	15.26	797
Grey	1	Horizontal I	8.1	8.03	8.08	8.06	15.36	15.18	15.28	778
	2	Horizontal II	8.07	7.99	8.11	8	15.26	15.17	15.18	757
	3	Horizontal III	8.16	8	8.14	8	15.31	15.22	15.2	768
	4	Horizontal IV	8.09	8.01	8.08	8.02	15.33	15.22	15.27	784
	5	Horizontal V	8.03	7.98	8.03	8.01	15.27	15.15	15.21	770
	6	Horizontal VI	8.1	8.01	8.08	8.03	15.37	15.26	15.29	778
	7	45° I	7.99	8.07	8.12	8.1	15.48	15.43	15.45	791
	8	45° II	7.96	8.02	8.09	8.1	15.48	15.41	15.45	787
	9	45° III	7.96	8.07	8.06	8.16	15.39	15.38	15.34	790
	10	45° IV	7.9	7.95	8.09	8.12	15.4	15.24	15.34	782
	11	45° V	7.98	8.1	8.06	8.17	15.42	15.35	15.27	784
	12	45° VI	7.98	7.95	8.12	8.16	15.37	15.36	15.34	795
	13	Vertical I	7.96	7.97	7.93	8	15.24	15.22	15.23	743
	14	Vertical II	8.04	8.05	8.05	8.03	15.27	15.25	15.25	739
	15	Vertical III	8.03	8.1	8.04	8.08	15.23	15.26	15.25	757
	16	Vertical IV	8.04	8.13	8.03	8.02	15.25	15.27	15.26	765
	17	Vertical V	8.07	8.03	8.03	7.99	15.26	15.26	15.25	753
	18	Vertical VI	8.05	8.13	8.1	8.07	15.23	15.3	15.23	754
Black	1	Horizontal I	7.98	8.02	7.96	8.03	15.22	15.14	15.2	749
	2	Horizontal II	8.05	8.04	8.02	8.01	15.24	15.18	15.19	765
	3	Horizontal III	8	8.01	7.98	8.05	15.22	15.17	15.2	761
	4	Horizontal IV	7.96	7.97	8.04	7.95	15.15	15.04	15.13	751
	5	Horizontal V	7.91	8.01	7.97	8.01	15.15	15.1	15.2	765
	6	Horizontal VI	7.96	8.01	7.96	7.99	15.1	15.05	15.09	748
	7	45° I	7.95	8.22	7.99	8.25	15.34	15.27	15.25	774
	8	45° II	7.91	8.21	7.97	8.18	15.39	15.31	15.27	780
	9	45° III	7.92	8.21	7.97	8.16	15.5	15.35	15.26	780
	10	45° IV	8	8.16	8	8.09	15.38	15.33	15.3	772
	11	45° V	7.9	8.11	8.05	8.29	15.34	15.24	15.21	773
	12	45° VI	7.93	8.2	8.02	8.12	15.4	15.34	15.36	765
	13	Vertical I	7.98	8.03	7.95	7.93	15.22	15.24	15.21	744
	14	Vertical II	7.9	7.9	7.89	7.94	15.24	15.26	15.24	738
	15	Vertical III	7.95	8.01	7.91	7.95	15.25	15.27	15.25	741
	16	Vertical IV	8.01	8.06	8.01	8.12	15.24	15.25	15.23	731
	17	Vertical V	8	7.97	7.98	7.94	15.24	15.24	15.24	715
	18	Vertical VI	8.04	8.03	7.95	7.98	15.21	15.26	15.28	739

basic dimensions were reported for diameter and length consecutively. Hanon et al. reviewed the dimensional accuracy of FDM 3D-printed cylindrical tribology test pieces made of bronze/PLA composite. An accuracy average of 99.65% for length and 98.19% for diameter was disclosed, which is in good agreement with the present study's results [22]. However, the weight showed a considerable variance among specimens produced in different conditions, as exhibited in Fig. 5. The diversity of colors has displayed a significant effect on the weight of the test pieces. The lightest weight was noticed in the black colored samples, where its weight average is 755 mg, no matter the print orientation. Whereas other color specimens have reported heavier weights, averaged 814 mg and 770.8 mg for the white and grey, respectively. Hence, the distinction between the heaviest (white) and lightest (black) specimens is almost a percentage of 7.24%. Furthermore, comparing the samples' weight for the same color, the 45° angle pieces offered the

Table 3
The raw results obtained from dimensional measurements of dog-bone test

Print parameter	No.	Sample settings	First point		Second point		Third point		Specimen weight (g)
			Width (mm)	Thickness (mm)	Width (mm)	Thickness (mm)	Width (mm)	Thickness (mm)	
Orientations	1	Flat I_45/135°_200 µm	10.07	3.9	10.05	3.98	9.99	4.05	9.57
	2	Flat II_45/135°_200 µm	10.18	3.9	10.05	3.97	9.96	4.08	9.49
	3	Flat III_45/135°_200 µm	10.05	3.94	10.01	4.03	9.99	4.05	9.54
	4	On-edge I_45/135°_200 µm	10.26	4.01	10.23	4.04	10.22	4.03	9.52
	5	On-edge II_45/135°_200 µm	10.23	4.01	10.23	4.06	10.2	4.03	9.65
	6	On-edge III_45/135°_200 µm	10.19	4.03	10.22	4.06	10.2	4.05	9.66
	7	Upright I_45/135°_200 µm	10	4	9.9	4.02	9.94	4.01	9.19
	8	Upright II_45/135°_200 µm	9.96	4.01	9.9	4	9.91	3.96	9.33
	9	Upright III_45/135°_200 µm	9.95	4.04	9.96	4	9.93	3.99	9.52
Raster direction	1	Flat_45/135° I_200 µm	10.07	3.9	10.05	3.98	9.99	4.05	9.57
	2	Flat_45/135° II_200 µm	10.18	3.9	10.05	3.97	9.96	4.08	9.49
	3	Flat_45/135° III_200 µm	10.05	3.94	10.01	4.03	9.99	4.05	9.54
	4	Flat_0/45° I_200 µm	9.94	4.12	9.95	4.02	9.95	3.96	9.65
	5	Flat_0/45° II_200 µm	10.02	4.05	10.09	4.03	10.1	3.92	9.6
	6	Flat_0/45° III_200 µm	9.96	4.09	9.93	4.04	9.92	3.99	9.6
	7	Flat_45/90° I_200 µm	9.93	4.1	9.92	3.99	9.93	3.91	9.62
	8	Flat_45/90° II_200 µm	9.92	3.87	9.91	3.96	9.87	3.99	9.55
	9	Flat_45/90° III_200 µm	9.93	4.05	9.95	3.98	9.91	3.92	9.41
Thickness	1	Flat_45/135°_200 µm I	10.07	3.9	10.05	3.98	9.99	4.05	9.57
	2	Flat_45/135°_200 µm II	10.18	3.9	10.05	3.97	9.96	4.08	9.49
	3	Flat_45/135°_200 µm III	10.05	3.94	10.01	4.03	9.99	4.05	9.54
	4	Flat_45/135°_100 µm I	9.87	3.92	9.85	3.83	9.87	3.75	9.49
	5	Flat_45/135°_100 µm II	9.89	3.8	9.86	3.75	9.87	3.65	9.2
	6	Flat_45/135°_100 µm III	9.83	3.88	9.88	3.79	9.87	3.72	9.35
	7	Flat_45/135°_300 µm I	9.97	3.71	9.93	3.65	9.94	3.56	7.77
	8	Flat_45/135°_300 µm II	9.91	3.74	9.97	3.69	9.92	3.62	7.96
	9	Flat_45/135°_300 µm III	10.01	3.75	9.98	3.7	9.99	3.61	7.75

Table 4
The average accuracy percentage obtained from dimensional measurements of cylindrical

Sample settings		Diameter (%)	SD (%)	Length (%)	SD (%)	Weight (%)	SD (%)
White	Horizontal	99.38	± 0.63	99.59	± 0.35	98.34	± 0.83
	45°	98.45	± 1.61	98.36	± 1.01	99.10	± 0.73
	Vertical	99.15	± 0.46	99.60	± 0.17	99.01	± 0.62
Grey	Horizontal	99.35	± 0.58	99.58	± 0.33	99.03	± 0.64
	45°	99.00	± 0.57	98.81	± 0.42	99.52	± 0.29
	Vertical	99.34	± 0.43	99.67	± 0.13	99.05	± 0.69
Black	Horizontal	99.63	± 0.25	99.64	± 0.33	99.06	± 0.23
	45°	98.61	± 1.03	99.19	± 0.45	99.49	± 0.45
	Vertical	99.38	± 0.43	99.72	± 0.12	98.95	± 0.85

highest values, while Horizontal and Vertical ones ranged more or less to the same extent.

3.3. Accuracy of dog-bone test specimens

A comparison among the dimensional (width and thickness) accuracy of dog-bone test specimens manufactured in different print orientation, raster direction, and layer thickness is exhibited in Fig. 6. High accuracy percentage was remarked for the width dimension in front of the basic (nominal) value. This accuracy reached higher than 99% for most tested samples, except the On-edge print orientation and the 100 µm layer thickness, where slight reductions were detected (97.85% and 98.66%, respectively). That indicates, there is no significant variation was recognized among the width measurements. This can be explained due to the fact that most of these specimens were printed in Flat print orientation, excluding the On-edge and Upright ones. As illustrated in Fig. 1 (b), the 3D printing process of any part includes building shell/wall (outer contour) and inner filling. The shell is the most robust part due to its larger thickness in the horizontal direction (wall thickness). Since the shell completely encloses the width measuring points of the Flat oriented samples. Thus, the width dimension shape error will be less even if the inner fill or layer thickness settings are different. This is due to the reliability of the outer contour, which is in contact with the measuring equipment. A similar interpretation could be attributed to the high accuracy of the Upright samples' width, as the shell is also the contact of the measuring points. Whereas for the case of On-edge printed specimens, the inner fill is the part which is in between the width measuring points. That means the number of layers is the important factor affecting the precision of the width here. Therefore, there was a reduction observed in the width accuracy of the On-edge pieces due to an elevated number of layers (width (10 mm) / layer thickness (0.2 mm) = 50 layers). In terms of dimensional thickness accuracy, a significant influence was obviously noticed in the layer

Table 5
The average accuracy percentage obtained from dimensional measurements of dog-bone (gauge section) tensile test samples.

Print settings		Width (%)	SD (%)	Thickness (%)	SD (%)	Weight (%)	SD (%)
Orientations	Flat	99.48	± 0.52	98.56	± 0.75	99.70	± 0.20
	On-Edge	97.85	± 0.20	99.12	± 0.46	99.38	± 0.28
	Upright	99.39	± 0.33	99.64	± 0.36	98.77	± 0.91
Raster direction	0/45°	99.38	± 0.25	98.69	± 0.88	99.77	± 0.10
	45/135°	99.48	± 0.52	98.56	± 0.75	99.70	± 0.20
	45/90°	99.19	± 0.22	98.54	± 1.07	99.19	± 0.51
Thickness	100 μm	98.66	± 0.17	94.69	± 2.06	98.96	± 0.87
	200 μm	99.48	± 0.52	98.56	± 0.75	99.70	± 0.20
	300 μm	99.56	± 0.31	91.75	± 1.60	98.87	± 0.49

thickness specimens. Theoretically, the greater the number of layers, the poor the dimensional accuracy [19]. Since the number of layers increases as the thickness of the layer decreases. Therefore,

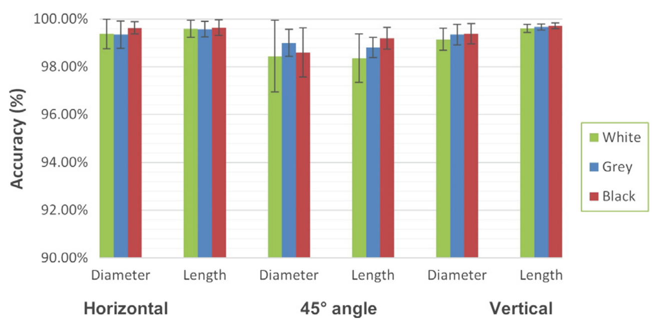

Fig. 4. Comparison among the average dimensional (diameter and length) accuracy of cylindrical test specimens manufactured in different print orientations and colors.

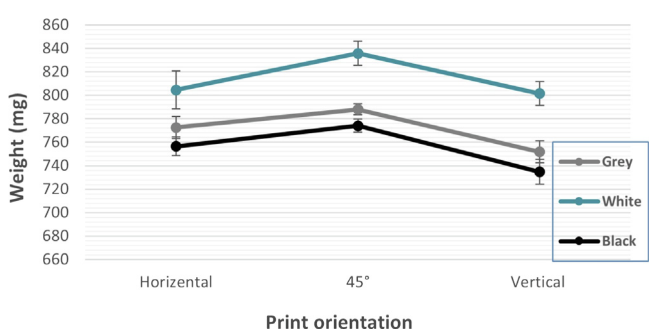

Fig. 5. Comparison among the average weight of cylindrical test specimens manufactured in different print orientations and colors.

it is conceivable that the 100 μm pieces present inferior thickness accuracy (around 94.69%) with a large error bar compared to the 200 μm (98.56%). As distorted growth becomes a dominant factor resulting from more layers, resulting in low dimensional precision [23]. Surprisingly, the 300 μm samples displayed the worst accuracy (91.75%) despite it supposed to be the best among the layer thickness ones, as its number of layers fewer. However, the reason behind it because the top layer is missing. For better understanding, the number of layers needed for forming the thickness of 300 μm specimen is calculated as following; specimen's thickness (4 mm) / thickness of layer (0.3 mm) = number of layers (13.33). The software will neglect this fraction of 0.33 because it did not reach 0.3 mm, as it equals only 0.1 mm. Consequently, the printer does not print a portion of this layer since the layer thickness was already set on a certain value. In connection with the effect of build orientation, all specimens (Flat, On-edge, and Upright) exhibited a high thickness accuracy percentage, ranging between 98.56% and 99.64%. In spite the shell of the On-edge and Upright specimens is the contact of thickness measuring points; nevertheless, the highest accuracy was observed in the Upright. This might be ascribed to the shell (contour) size of the whole piece. As the small size of the contour decreases shrinkage and improves precision [22]. Accordingly, the Upright's thickness accuracy enhanced since its contour size for each layer is much smaller than the contour of On-edge samples. Unlike other print parameters, raster direction angle specimens showed almost the same range of thickness accuracy percentage (98.54% – 98.69%). This implies that the raster direction angle has no impact on the thickness accuracy when the number of layers and the contour size are the same. As an average dimensional accuracy for dog-bone specimens regardless of the printing settings, a percentage of 99.16% for width and 97.57% for thickness were obtained compared to the nominal values. This high dimensional accuracy rate would agree with the findings of Alsoufi et al., where the dimensional accuracy of PLA thermoplastic material in a rectangular form was evaluated. They

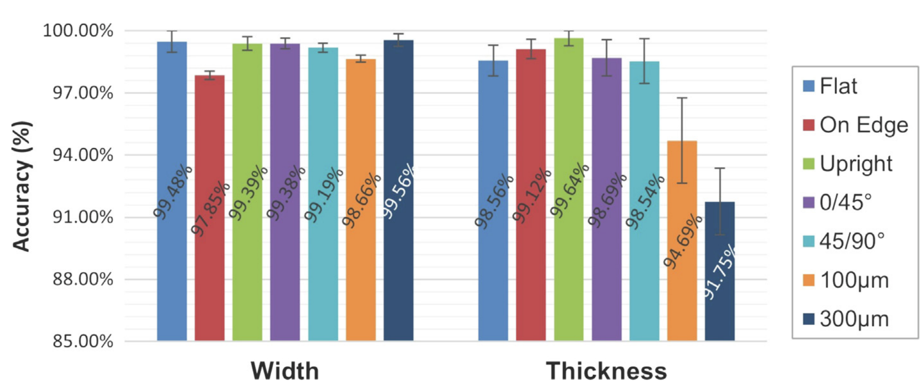

Fig. 6. Comparison among the average dimensional (width and thickness) accuracy of dog-bone test specimens manufactured in different print orientation, raster direction, and layer thickness.

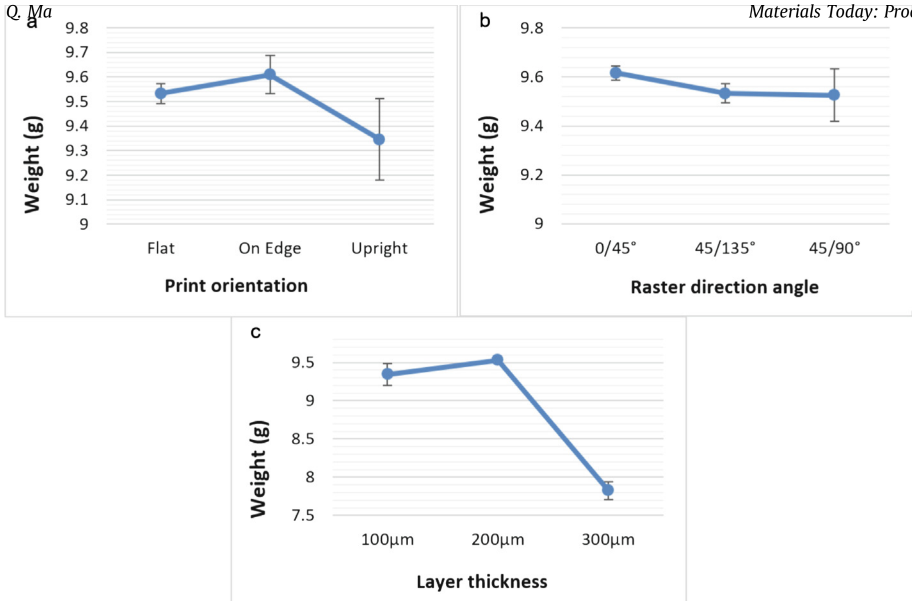

Fig. 7. Comparison among the average weight of dog-bone test specimens manufactured in different (a) print orientation; (b) raster direction angle, and (c) layer thickness.

indicated that shape error variation on all specimens' faces had not exceeded 3.00% due to the less occurrence of warping deformation than other materials examined in their research [18].

Eventually, a processing accuracy of 98.81% was gained in the current work through the overall average dimensional precision for both cylindrical (diameter and length) and dog-bone (width and thickness) samples.

A comparison among the average weight of dog-bone test specimens manufactured in different print orientation, raster direction angle, and layer thickness is presented in Fig. 7. A slight reduction was observed for the weight of the Upright test piece (9.34 g) as compared to the other print orientations (Flat (9.53 g) and 45° angle (9.61 g)), which are almost similar (see Fig. 7 (a)). Further, no significant difference was noticed among raster direction angle specimens (Fig. 7 (b)), as all of them averaged within the same range (between 9.52 g and 9.61 g). On the other hand, Fig. 7 (c) shows a notable reduction of $\sim$17.9% in the weight of the 300 μm pieces against the weight of other layer thicknesses (9.34 g for 100 μm and 9.53 g for 200 μm), which were approximately alike. This reduction could be simply attributed to the top layer missing, as has been aforementioned.

4. Conclusions

This study analyzed the dimensional and weight accuracy of 3D-printed PLA material in three different colors. The experiment comprised the dimensional accuracy evaluation for cylindrical (diameter and length) and dog-bone tensile test (width and thickness of the gauge section) specimens. The weight precision was also examined for both the mentioned samples. The following conclusions have been drawn based on the observations:

- Commercial desktop FDM 3D printers could be used as an inexpensive and decent quality alternative for producing utilitarian parts with a high processing accuracy of 98.81% when investigated pieces compared to the nominal dimensions.
- The worst dimensional accuracy for cylindrical specimens (diameter and length) with elevated standard deviation error bars was observed in the 45° angle sample due to tilted layers positioning when models are constructed, as the influence of gravity increases distortion.
- Generally, most cylindrical samples reported high accuracy percentage since overall calculations ranged as 99.14% and 99.35% for diameter and length consecutively against the basic dimensions.
- The filament color displayed a considerable effect on the test pieces' weight, where the distinction between the heaviest (white) and lightest (black) specimens is almost a percentage of 7.24%.
- For the dog-bone samples, high accuracy and no significant variation were detected among Flat and Upright's width measurements because the shell completely encloses measuring points. In contrast, On-edge exhibited a slight reduction due to inner filling is the contact of width measuring points where the number of layers becomes the dominant factor.
- A remarkable influence was noticed for the layer thickness parameter. The 100 μm pieces presented inferior thickness accuracy (94.69%) with a large error bar compared to the 200 μm (98.56%). As distorted growth becomes a prevailing factor as a result of more layers, resulting in low dimensional precision. An exception was detected in the 300 μm sample. It revealed the worst accuracy (91.75%) because the top layer is missing due to not reaching the correct value for the specified layer thickness (300 μm). Hence, the fraction value is neglected.
- All build orientation specimens exhibited a high thickness accuracy percentage, ranging between 98.56% and 99.64%. The highest value was offered by the Upright since its contour size for each layer is much smaller than on-edge samples. As the small size of the contour decreases shrinkage and improves precision.
- The raster direction angle parameter appeared no impact on the thickness accuracy when the number of layers and the contour size are the same.
- A notable reduction of $\sim$17.9% in the weight of the dog-bone pieces with a thickness of 300 μm versus 100 μm (9.34 g) and 200 μm (9.53 g) could be attributed to the missing upper layer.
- Finally, the best overall dimensional accuracies were obtained with the printing settings of "black color/Horizontal build orientation/[45/135°] raster angle/200 μm layer thickness, (99.63%)" and "black color/Vertical build orientation/[45/135°] raster angle/200 μm layer thickness, (99.72%)" for diameter and length of cylindrical specimens, respectively, as well as "Flat build orientation/[45/135°] raster angle/300 μm layer

thickness, (99.56%)" and "Upright build orientation/[45/135°] raster angle/200 μm layer thickness, (99.64%)" for width and thickness of the dog-bone samples, consecutively.

To sum up, 3D printed parts' dimensional accuracy could be improved within the desired range by appropriately controlling the machine process parameters.

Declaration of Competing Interest

The authors declare that they have no known competing financial interests or personal relationships that could have appeared to influence the work reported in this paper.

Acknowledgements

This work was supported by the Stipendium Hungaricum Programme and by the Mechanical Engineering Doctoral School, Szent István University, Gödöllő, Hungary.

References

[1] N. Ayrilmis, M. Kariz, J.H. Kwon, M. Kitek Kuzman, Effect of printing layer thickness on water absorption and mechanical properties of 3D-printed wood/PLA composite materials, Int. J. Adv. Manuf. Technol. 102 (5-8) (2019) 2195–2200, https://doi.org/10.1007/s00170-019-03299-9.

[2] J.M. Pearce, Applications of Open Source 3-D Printing on Small Farms, Org. Farming. 1 (2015). 10.12924/of2015.01010019.

[3] J. Zuniga, D. Katsavelis, J. Peck, J. Stollberg, M. Petrykowski, A. Carson, C. Fernandez, Cyborg beast: a low-cost 3d-printed prosthetic hand for children with upper-limb differences, BMC Res. Notes. 8 (2015) 10, https://doi.org/10.1186/s13104-015-0971-9.

[4] H. Bikas, P. Stavropoulos, G. Chryssolouris, Additive manufacturing methods and modelling approaches: a critical review, Int. J. Adv. Manuf. Technol. 83 (1-4) (2016) 389–405, https://doi.org/10.1007/s00170-015-7576-2.

[5] B. Esmaeilian, S. Behdad, B. Wang, The evolution and future of manufacturing: A review, J. Manuf. Syst. 39 (2016) 79–100, https://doi.org/10.1016/j.jmsy.2016.03.001.

[6] H. Rezayat, W. Zhou, A. Siriruk, D. Penumadu, S.S. Babu, Structure–mechanical property relationship in fused deposition modelling, Mater. Sci. Technol. 31 (8) (2015) 895–903, https://doi.org/10.1179/1743284715Y.0000000010.

[7] Z. Weng, J. Wang, T. Senthil, L. Wu, Mechanical and thermal properties of ABS/montmorillonite nanocomposites for fused deposition modeling 3D printing, Mater. Des. 102 (2016) 276–283, https://doi.org/10.1016/j.matdes.2016.04.045.

[8] T. Serra, J.A. Planell, M. Navarro, High-resolution PLA-based composite scaffolds via 3-D printing technology, Acta Biomater. 9 (3) (2013) 5521–5530, https://doi.org/10.1016/j.actbio.2012.10.041.

[9] M.M. Hanon, R. Marczis, L. Zsidai, Anisotropy Evaluation of Different Raster Directions, Spatial Orientations, and Fill Percentage of 3D Printed PETG Tensile Test Specimens, Key Eng. Mater. 821 (2019) 167–173, https://doi.org/10.4028/www.scientific.net/KEM.821.167.

[10] J.T. Cantrell, S. Rohde, D. Damiani, R. Gurnani, L. DiSandro, J. Anton, A. Young, A. Jerez, D. Steinbach, C. Kroese, P.G. Ifju, Experimental characterization of the mechanical properties of 3D-printed ABS and polycarbonate parts, Rapid Prototyp. J. 23 (4) (2017) 811–824, https://doi.org/10.1108/RPJ-03-2016-0042.

[11] M. Rybachuk, C. Alice Mauger, T. Fiedler, A. Öchsner, Anisotropic mechanical properties of fused deposition modeled parts fabricated by using acrylonitrile butadiene styrene polymer, J. Polym. Eng. 37 (2017), https://doi.org/10.1515/polyeng-2016-0263.

[12] Z. Liu, Y. Wang, B. Wu, C. Cui, Y.u. Guo, C. Yan, A critical review of fused deposition modeling 3D printing technology in manufacturing polylactic acid parts, Int. J. Adv. Manuf. Technol. 102 (9-12) (2019) 2877–2889, https://doi.org/10.1007/s00170-019-03332-x.

[13] A.C. Abbott, G.P. Tandon, R.L. Bradford, H. Koerner, J.W. Baur, Process-structure-property effects on ABS bond strength in fused filament fabrication, Addit. Manuf. 19 (2018) 29–38, https://doi.org/10.1016/j.addma.2017.11.002.

[14] Z. Quan, J. Suhr, J. Yu, X. Qin, C. Cotton, M. Mirotznik, T.-W. Chou, Printing direction dependence of mechanical behavior of additively manufactured 3D preforms and composites, Compos. Struct. 184 (2018) 917–923, https://doi.org/10.1016/j.compstruct.2017.10.055.

[15] Q. Ma, M. Rejab, A.P. Kumar, H. Fu, N.M. Kumar, J. Tang, Effect of infill pattern, density and material type of 3D printed cubic structure under quasi-static loading 095440622097166 Proc. Inst. Mech. Eng. Part C J. Mech. Eng. Sci. (2020), https://doi.org/10.1177/0954406220971667.

[16] M.M. Hanon, R. Marczis, L. Zsidai, Influence of the 3D Printing Process Settings on Tensile Strength of PLA and HT-PLA, Period. Polytech. Mech. Eng. (2020), https://doi.org/10.3311/PPme.13683.

[17] D. Hyndhavi, G.R. Babu, S.B. Murthy, Investigation of Dimensional Accuracy and Material Performance in Fused Deposition Modeling, Mater. Today Proc. 5 (11) (2018) 23508–23517, https://doi.org/10.1016/j.matpr.2018.10.138.

[18] M.S. Alsoufi, A.E. Elsayed, Surface Roughness Quality and Dimensional Accuracy—A Comprehensive Analysis of 100% Infill Printed Parts Fabricated by a Personal/Desktop Cost-Effective FDM 3D Printer, Mater. Sci. Appl. 09 (2018) 11–40, https://doi.org/10.4236/msa.2018.91002.

[19] Z.-C. Zhang, P.-L. Li, F.-T. Chu, G. Shen, Influence of the three-dimensional printing technique and printing layer thickness on model accuracyEinfluss der dreidimensionalen Drucktechnik und Schichtstärke auf die Modellgenauigkeit, J. Orofac. Orthop. / Fortschritte Der Kieferorthopädie. 80 (4) (2019) 194–204, https://doi.org/10.1007/s00056-019-00180-y.

[20] P.J. Nuñez, A. Rivas, E. García-Plaza, E. Beamud, A. Sanz-Lobera, Dimensional and Surface Texture Characterization in Fused Deposition Modelling (FDM) with ABS plus, Procedia Eng. 132 (2015) 856–863, https://doi.org/10.1016/j.proeng.2015.12.570.

[21] International Organization for Standardization, ISO 527-2:2012: Plastics - Determination of tensile properties - Part 2: Test conditions for moulding and extrusion plastics, 2012. https://www.iso.org/standard/56046.html.

[22] M.M. Hanon, Y. Alshammas, L. Zsidai, Effect of print orientation and bronze existence on tribological and mechanical properties of 3D-printed bronze/PLA composite, Int. J. Adv. Manuf. Technol. 108 (1-2) (2020) 553–570, https://doi.org/10.1007/s00170-020-05391-x.

[23] O.A. Mohamed, S.H. Masood, J.L. Bhowmik, M. Nikzad, J. Azadmanjiri, Effect of Process Parameters on Dynamic Mechanical Performance of FDM PC/ABS Printed Parts Through Design of Experiment, J. Mater. Eng. Perform. 25 (7) (2016) 2922–2935, https://doi.org/10.1007/s11665-016-2157-6.